Form factor fits

Jonathan Flynn

Physics & Astronomy
University of Southampton

Flavour@TH 8–12 May 2023

Introduction

- Mainly concerned with semileptonic heavy-to-light decays from lattice perspective
- … where there is a long extrapolation to cover the physical range of q^2, squared momentum-transfer to the leptons,
- …including the low-q^2 region where experimental data is most precise

Semileptonic heavy-to-light meson decay on the lattice

L^{-1}		a^{-1}
finite box	$\ll$ physics of interest $\ll$	lattice spacing

Kinematics: example $B \longrightarrow \pi l \nu$

$$q^2_{\text{max}} = (m_B - m_\pi)^2 \approx 26.4\,\text{GeV}^2$$

Lowest Fourier modes on $L = 4$ fm lattice

$\lvert\vec{n}^2\rvert$	0	1	2	3	4
E_π / GeV	0.139	0.338	0.457	0.551	0.631
q^2 / GeV^2	26.4	24.3	23.1	22.1	21.2

Limited coverage of q^2 range

RBC-UKQCD PRD91 074510 2015[1]

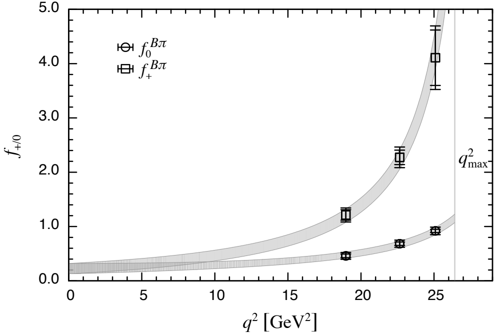

Exploiting dispersion relations to control q^2 extrapolation

Okubo PRD3 2897 1971[2], PRD4 725 1971[3]; Okubo and Shih PRD4 2020 1971[4]; Bourrely, Machet, de Rafael NPB189 157 1981[5]; Boyd, Grinstein, Lebed PLB353 306 1995[6], NPB461 493 1996[7], PRD56 6895 1997[8]; Lellouch NPB479 353 1996[9]

Extrapolation in q^2, z transformation

- Unitarity/analyticity bounds via dispersion relation $\longrightarrow$ fast-converging model-independent series expansion in z

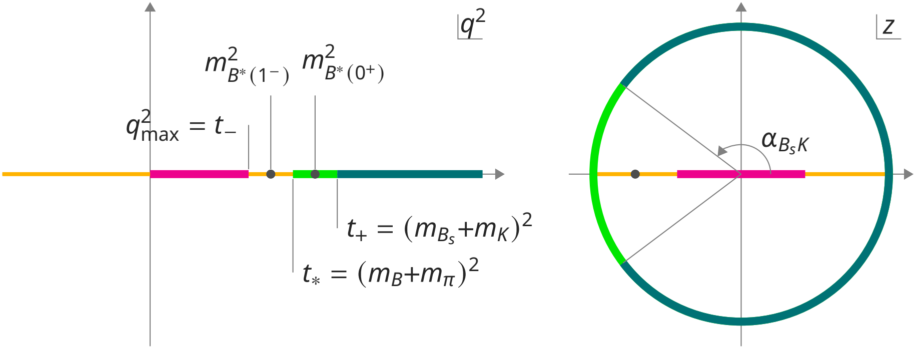

- Illustrated for $B_s \to K$ where start of cut and threshold for B_sK production differ
- Integrate over arc of unit circle $[-\alpha_{B_sK}, \alpha_{B_sK}]$ where $\alpha_{B_sK} = \arg[z(t_+)]$

Gubernari et al 2021, 2022[10,11], Blake et al 2022[12]

BGL expansion

$$f_X(q_i^2) = \frac{1}{B_X(q_i^2)\phi_X(q_i^2)} \sum_{n=0}^{K_X-1} a_{X,n}\, z(q_i^2)^n = Z_{XX,in} a_{X,n}$$

Two constraints

- Kinematic: $f_+(0) = f_0(0)$ (eliminates one of the $a_{X,n}$)
- Unitarity:

$$\frac{1}{2\pi i} \oint_{|z|=1} \frac{dz}{z}\, \theta_\alpha \left| B_X(q^2)\phi_X(q^2) f_X(q^2) \right|^2 \leq 1$$

where $\theta_\alpha = \theta\big(\alpha - |\arg(z)|\big)$

$$a_{X,i} \langle z^i | z^j \rangle_\alpha a_{X,j} \leq 1$$

$$\langle z^i | z^j \rangle_\alpha = \frac{1}{2\pi} \int_{-\alpha}^{\alpha} d\phi\, (z^*)^i z^j \Big|_{z=e^{i\phi}} = \begin{cases} \frac{\sin(\alpha(i-j))}{\pi(i-j)} & i \neq j\,, \\ \frac{\alpha}{\pi} & i = j \end{cases}$$

JF, Jüttner, Tsang 2303.11285[13]

BGL: frequentist fit

Input (eg lattice ff)

$$\mathbf{f}^T = (\mathbf{f}_+, \mathbf{f}_0)^T$$
$$= \big(f_+(q_0^2), f_+(q_1^2), \ldots, f_+(q_{N_+-1}^2), f_0(q_0^2), f_0(q_1^2), \ldots, f_0(q_{N_0-1}^2)\big)$$

Output (BGL params)

$$\mathbf{a}^T = (\mathbf{a}_+, \mathbf{a}_0)^T = (a_{+,0}, a_{+,1}, \ldots, a_{+,K_+-1}, a_{0,1}, a_{0,2}, \ldots, a_{0,K_0-1})$$

Frequentist fit

$$\chi^2(\mathbf{a}, \mathbf{f}) = (\mathbf{f} - Z\mathbf{a})^T C_{\mathbf{f}}^{-1} (\mathbf{f} - Z\mathbf{a})$$

Frequentist result

$$\mathbf{a} = (Z^T C_{\mathbf{f}}^{-1} Z)^{-1} Z C_{\mathbf{f}}^{-1} \mathbf{f}, \qquad C_{\mathbf{a}} = (Z^T C_{\mathbf{f}}^{-1} Z)^{-1}$$

- Z contains BGL ansatz and kinematic constraint
- Written here using constraint to eliminate $a_{0,0}$:

$$a_{0,0} = \frac{B_0(0)\phi_0(0)}{B_+(0)\phi_+(0)} \sum_{k=0}^{K_+-1} a_{+,k} z(0)^k - \sum_{k=1}^{K_0-1} a_{0,k} z(0)^k$$

Frequentist fit practicalities

- Truncation: limited number of (synthetic) input form-factor points, plus kinematic constraint, limits number of terms in z-expansion

$$K_+ + K_0 - 1 < N_+ + N_0$$

- Truncation of series shows up in:
  - Varying locations of the synthetic points shows large variation in $f_{+,0}(0)$ values
  - Varying t_0 in z-transformation shows large variation in $f_{+,0}(0)$ values

Functional matching FNAL-MILC PRD92 014024 2015[14], FNAL-MILC PRD100 034501 2019[15]

- Lattice calculation typically gives a parametrised function for a form factor over a limited range, often linear in the parameters

$$f_{\text{lat}}(z) = c_i \phi_i(z) \qquad z_1 \le z \le z_2$$

- You know the covariance of $f_{\text{lat}}(z)$ and $f_{\text{lat}}(z')$

$$K(z,z') = \text{cov}\big(f_{\text{lat}}(z) f_{\text{lat}}(z')\big) = \phi_i(z)\text{cov}(c_i c_j)\phi_j(z')$$

- Match to z-expansion (eg BGL or BCL ▸ BCL), $f(z,\mathbf{a})$, in $z_1 \le z \le z_2$ by minimising

$$\chi^2_{\text{lat}} = \int_{z_1}^{z_2} dz \int_{z_1}^{z_2} dz' \, [f_{\text{lat}}(z) - f(z,\mathbf{a})] K^{-1}(z,z') [f_{\text{lat}}(z') - f(z',\mathbf{a})]$$

- Limited number of parameters c_i shows up as zero eigenvalues of the linear operator defined by $K(z,z')$
- Regulate by discarding singular modes before inverting K

Functional matching: $B_s \to K\ell\nu$

FNAL-MILC PRD100 034501 2019[15]

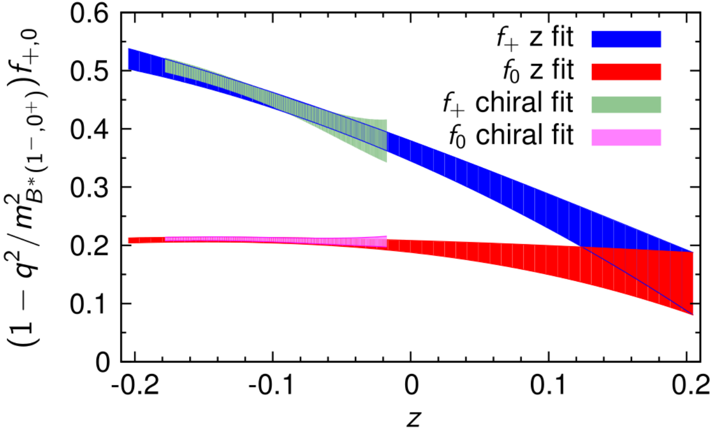

- BCL z-fits with $K_{+,0} = 4$ and kinematic constraint
- χ^2_{lat}'s frequentist interpretation unclear

Dispersive matrix bounds

- determine $f(t)$ with $f(t_i)$ known at positions t_i ($t = q^2$)
- let $F(t) = B(t)\phi(t)f(t)$ and write $F^{\mathrm{T}} = (F_0, F_1, \ldots, F_N)$ with $F_0 = F(t)$ and $F_i = F(t_i)$
- define inner product

$$\langle g|h\rangle = \frac{1}{2\pi i}\int_{|z|=1} \bar{g}(z)h(z)$$

and

$$g_t(z) \equiv \frac{1}{1-\bar{z}(t)z} \quad \text{with} \quad \langle g_t|h\rangle = h(t)$$

- build Gram matrix M of inner products of $F, g_t, g_{t_1}, g_{t_2}, \ldots, g_{t_N}$

$$M = \begin{bmatrix} \langle F|F\rangle & F^{\mathrm{T}} \\ F & G \end{bmatrix}$$

- G is Gram matrix of inner products of $g_t, g_{t_1}, \ldots, g_{t_N}$
- $\det M = \det G \times (\langle F|F\rangle - F^{\mathrm{T}}G^{-1}F) \geq 0$ with $\det G \geq 0$.
- dispersion relation $\langle F|F\rangle \leq \chi$ gives

$$\chi - F^{\mathrm{T}}G^{-1}F \geq 0$$

quadratic inequality for F_0 and hence $f(t)$

Dispersive matrix method results

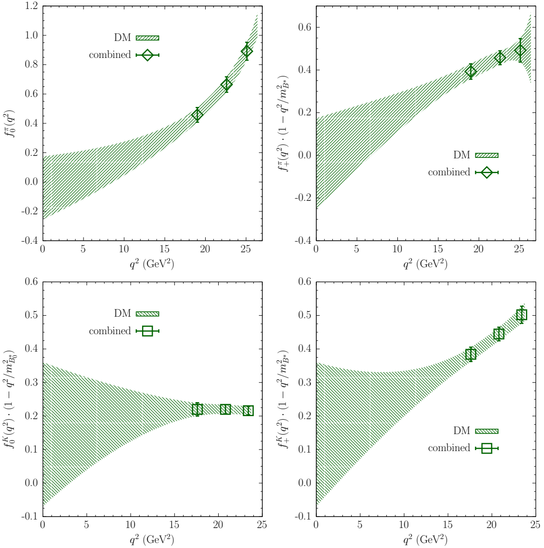

- plots from JHEP 08 022 2022[16]
  top: $B \longrightarrow \pi$ RBC-UKQCD 15[1] FNAL-MILC 15[14]
  bottom: $Bs \longrightarrow K$ HPQCD 14[17], RBC-UKQCD 15[1], FNAL-MILC 19[15]
- χ's from lattice-computed current-current correlators
- indirect implementation of kinematic constraint
- use input data from different sources by combining form-factors at common q^2 points
- lacks frequentist interpretation

Di Carlo et al PRD104 054502 2021[18]; Martinelli et al PRD104 094512 2021[19], PRD105 034503 2022[20], JHEP 08 022 2022[16], PRD106 093002 2022[21]

$f_+(0) = f_0(0)$ constraint in DM method

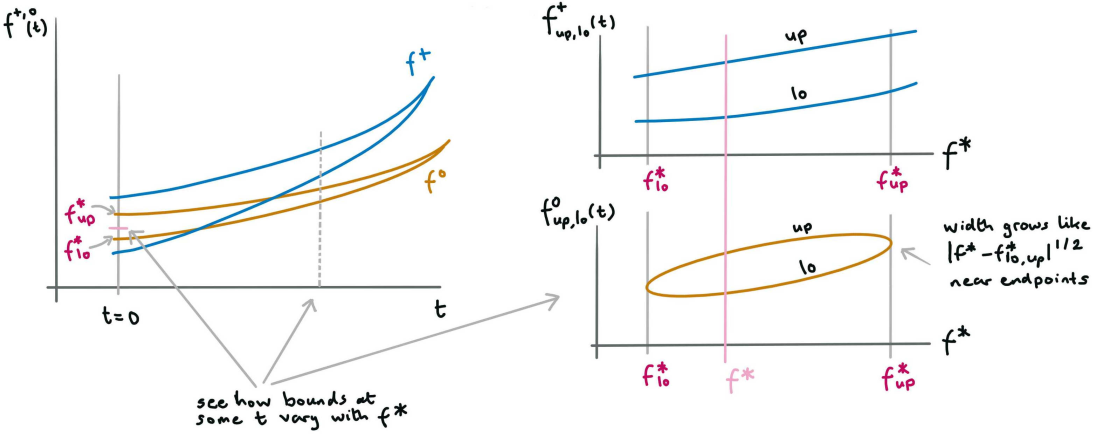

$f_+(0) = f_0(0)$ constraint in DM method 2

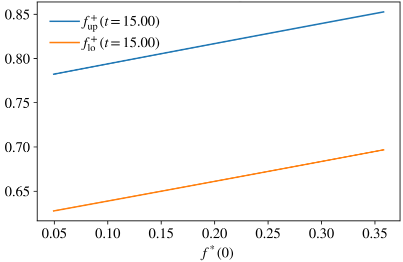

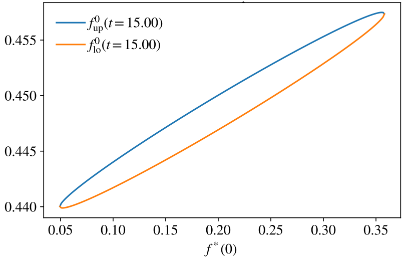

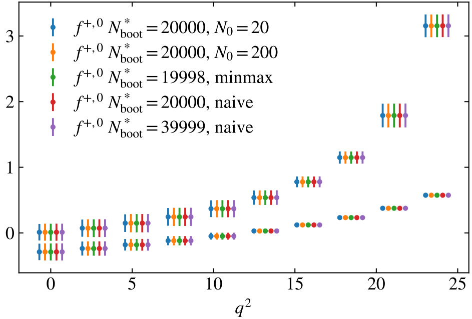

- left: variation of upper and lower bounds for $f_{+,0}(15\,\text{GeV}^2)$ for $f^*_{lo} \le f^* \le f^*_{up}$
- above: $f_{+,0}$ bounds for different treatments of inner bootstrap. f_0 points shifted down to separate them from f_+ at low q^2

Bayesian BGL form factor fit

- Frequentist fit
  - $N_{\mathrm{dof}} = N_{\mathrm{data}} - N_{\mathrm{params}} \geq 1$ means in practice truncation of z expansion at low order
  - induced systematic
- Bayesian fit [RBC-UKQCD 2303.11280[22]; JF, Jüttner, Tsang 2303.11285[13]]
  - aim to fit full z expansion (no truncation)
  - need regulator to control higher-order coefficients — use unitarity constraint
  - compute (functions of) z-expansion coefficients as expectation values

$$\langle g(\mathbf{a})\rangle = N \int d\mathbf{a}\, g(\mathbf{a})\, \pi(\mathbf{a}|\mathbf{f}, C_{\mathbf{f}})\, \pi_{\mathbf{a}}$$

with probability for parameters given model and data

$$\pi(\mathbf{a}|\mathbf{f}, C_{\mathbf{f}}) \propto \exp\left(-\frac{1}{2}\chi^2(\mathbf{a},\mathbf{f})\right) \qquad \text{where} \qquad \chi^2(\mathbf{a},\mathbf{f}) = (\mathbf{f} - Z\mathbf{a})^T C_{\mathbf{f}}^{-1} (\mathbf{f} - Z\mathbf{a})$$

and prior knowledge from unitarity constraint

$$\pi_{\mathbf{a}} \propto \theta\left(1 - |\mathbf{a}_+|_\alpha^2\right)\, \theta\left(1 - |\mathbf{a}_0|_\alpha^2\right)$$

Bayesian BGL form factor fit

- use MC integration: sample $\mathbf{a}$ from multivariate normal and drop samples incompatible with unitarity
- in practice, low probability to satisfy unitarity when K_+ and K_0 large
- modify

$$\pi(\mathbf{a}|\mathbf{f}_p, C_{\mathbf{f}_p})\, \pi_{\mathbf{a}}(\mathbf{a}_p|M) \propto \theta(\mathbf{a})\ \exp\left(-\frac{1}{2}(\mathbf{f}_p - Z\mathbf{a})^T C_{\mathbf{f}_p}^{-1}(\mathbf{f}_p - Z\mathbf{a}) - \frac{1}{2}\mathbf{a}^T \frac{M}{\sigma^2}\mathbf{a}\right)$$

  - choose M such that $\mathbf{a}^T M\mathbf{a} \leq 2$ in presence of kinematic constraint
  - draw random number
  - correct with accept-reject with probability

$$p \leq \frac{\exp(-1/\sigma^2)}{\exp(-\mathbf{a}^T \frac{M}{2\sigma^2}\mathbf{a})}$$

Example: $B_s \longrightarrow K\ell\nu$

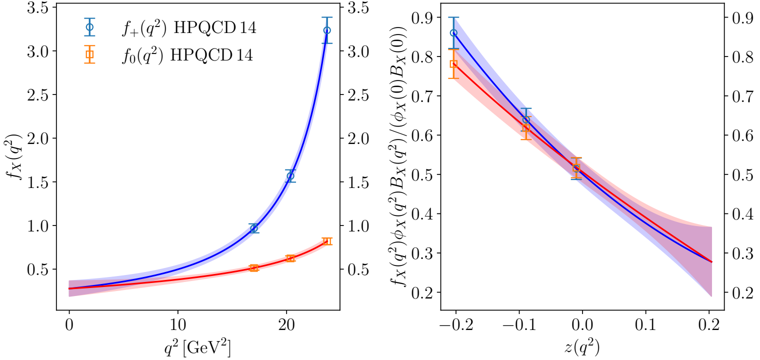

Bayesian $(K_+, K_0) = (5, 5)$ fit for HPQCD 14 data

HPQCD PRD90 054506 2014[17]

- Frequentist and Bayesian agree when comparison possible
- Frequentist provides *p*-value; no quality of fit for Bayesian
- Unitarity constraint stabilises higher orders $\longrightarrow$ BGL fit without truncation ▸ coeffts
- Stat error on low-order coeffts a little larger than for low-order frequentist fit (Bayes allows more freedom in functional form)

Easy to combine data: $B_s \longrightarrow K\ell\nu$

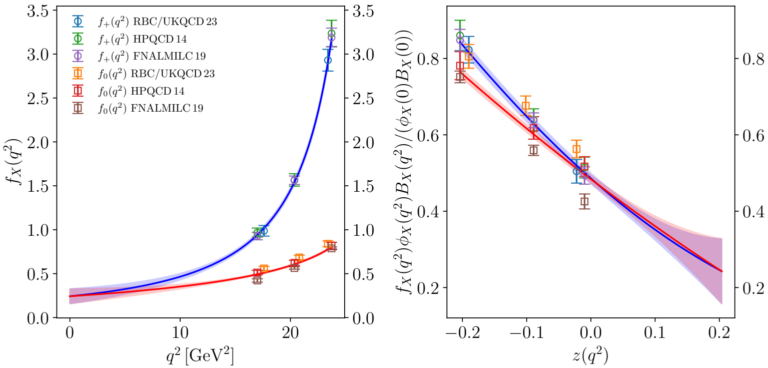

Bayesian $(K_+, K_0) = (5, 5)$ fit for HPQCD 14, FNAL-MILC 2019 and RBC-UKQCD 23 data

HPQCD PRD90 054506 2014[17]

FNAL-MILC PRD100 034501 2019[15]

RBC-UKQCD 2303.11280[22]

- Bayesian and frequentist provide complementary information; consider both ▸ Freq fit

Combine with non-lattice data: eg sum rules, experiment

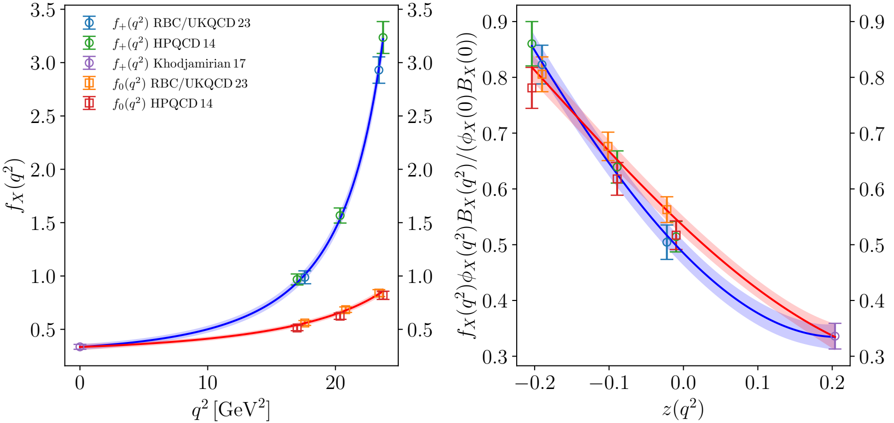

Bayesian $(K_+, K_0) = (5, 5)$ fit for HPQCD 14, RBC-UKQCD 23 and sum rule data

HPQCD PRD90 054506 2014[17], RBC-UKQCD 2303.11280[22], Khodjamirian, Rusov JHEP 08 112 2017[23]

Relation to dispersive matrix approach

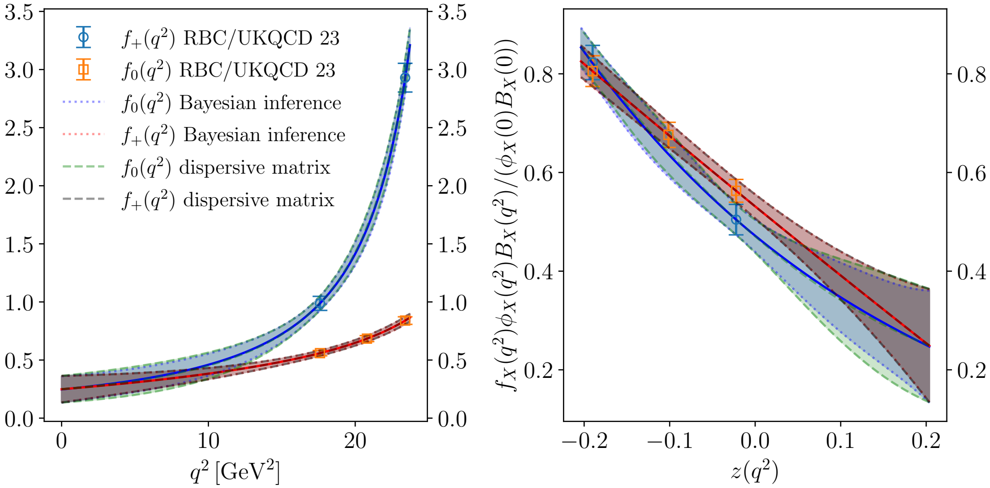

Bayesian inference and dispersive matrix approach applied to our own data

RBC-UKQCD 2303.11280[22]

$B \to \pi l \nu$

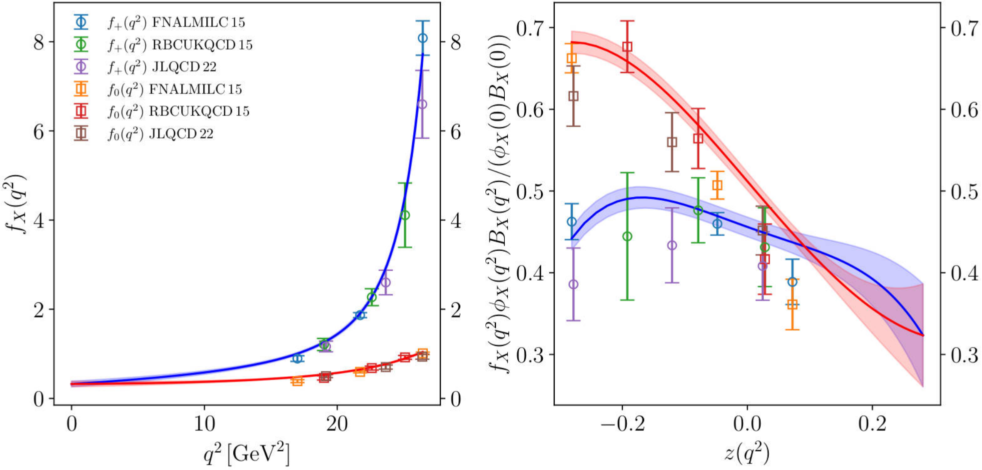

FNAL-MILC PRD92 014024 2015[14], RBC-UKQCD PRD91 074510 2015[1], JLQCD PRD106 054502 2022[24]

Self-consistency in z-expansions Simons, Gustafson, Meurice 2304.13045[26]

- Perfect knowledge of an analytic function on one part of real axis uniquely determines it on another part
- Extend (approximate) polynomial determined in high-z region to all z: $f^{\text{high}}(z)$. Similarly for for low-z region: $f^{\text{low}}(z)$.
- Use discrepancy $f^{\text{high}}(z) - f^{\text{low}}(z)$ over some range of z to devise a measure of self-consistency

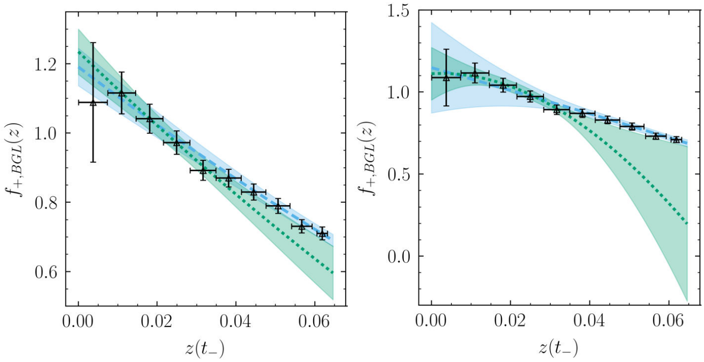

- 2nd (left) or 3rd (right) order fits to z polys in BGL fits to Belle $B \longrightarrow D$ data PRD93 032006 2016[25]
- blue: high-z fit, green: low-z fit

$B_s \to K\ell\nu$: extrapolation of lattice data

$$f_X(E_K, m_\pi, a) = \frac{1}{E_K + \Delta_X}\left(d_{X,0} + c_{X,1}E_K + c_{X,2}E_K^2 + d_{X,1}a^2 + d_{X,2}L(m_\pi)\right)$$

- $\Delta = m_{B^*} - m_{B_s}$ where m_B^* is $\bar{b}u$ flavour state with $J^P = 1^-(0^+)$ for $f_+(f_0)$
- Form factors $f_{\|,\perp}$ easier to extract on lattice

$$f_+(q^2) = \frac{1}{\sqrt{2m_{B_s}}}\left[f_\|(E_K) + (m_{B_s} - E_K)f_\perp(E_K)\right]$$

$$f_0(q^2) = \frac{\sqrt{2m_{B_s}}}{m_{B_s}^2 - m_K^2}\left[(m_{B_s} - E_K)f_\|(E_K) + (E_K^2 - m_K^2)f_\perp(E_K)\right]$$

- Chiral/continuum extrapolation in the past done for $f_{\|,\perp}$, then converted, assuming $f_{\|(\perp)}$ dominated by $f_{0(+)}$. FNAL-MILC PRD100 034501 2019[15], RBC-UKQCD PRD91 074510 2015[1]
- Now chiral/continuum extrapolation for $f_{+,0}$ RBC-UKQCD 2303.11280[22]

$B_s \to K\ell\nu$: extrapolation of lattice data 2

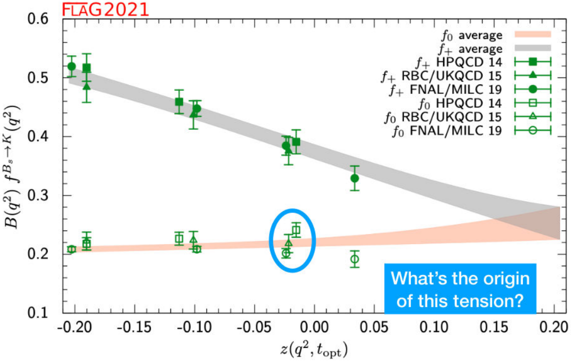

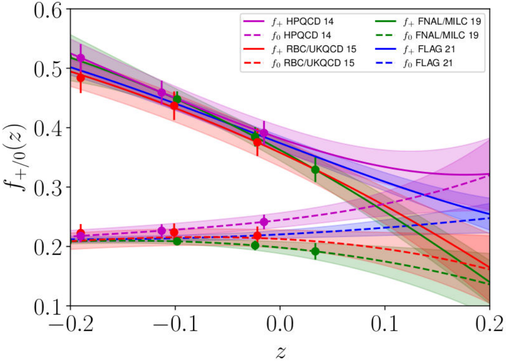

- $f_{\|,\perp}$ vs $f_{+,0}$ makes a difference at low q^2 in RBC-UKQCD 23[22] data
- Helps explain differences in subsequent extrapolations to $q^2 = 0$?

Summary

- Aim for truncation-independence in z fits
- Bayesian inference
  - unitarity constraint built in
  - kinematic constraint directly implemented
  - easy to combine theory and experimental input
  - easy-to-use output (a set of BGL z-fit coefficients and their correlations)

Backup

z transformation

Let $t = q^2$

$$z(t; t_*, t_0) = \frac{\sqrt{t_* - t} - \sqrt{t_* - t_0}}{\sqrt{t_* - t} + \sqrt{t_* - t_0}}.$$

- Maps $q^2 = t$ plane, with cut along $t \geq t_*$, onto disk $|z| < 1$
- t_* is threshold for two-particle production for lowest-mass two-particle state with correct quantum numbers
- Transformation takes cut $t_* \leq t < \infty$ onto $|z| = 1$ and takes $t_* > t > -\infty$ onto $(-1, 1)$
- $z(t_0; t_*, t_0) = 0$. Choose t_0 to fix range of z corresponding to $0 \leq q^2 = t \leq t_-$
- To symmetrize z-range around the origin:

$$t_0 = t_* - \sqrt{t_*(t_* - t_-)}$$

BCL parametrisation Bourrely, Caprini, Lellouch PRD79 013008 2009[27]

$$f_+(q^2) = \frac{1}{1 - q^2/m^2_{B^*(1^-)}} \sum_{k=0}^{K_+-1} b_k^+ \left[z^k - (-1)^k - K_+ \frac{k}{K_+} z^{K_+} \right]$$

$$f_0(q^2) = \frac{1}{1 - q^2/m^2_{B^*(0^+)}} \sum_{k=0}^{K_0-1} b_k^0 z^k$$

- $1/(1 - q^2/m^2_{B^*(1^-)})$ in f_+ accounts for sub-threshold pole
- pole factors ensure $f(q^2) \sim 1/q^2$ at large q^2
- ensure correct threshold behaviour near start of cut for f_+
- form used in FNAL-MILC PRD100 034501 2019[15]

◂ func match

HPQCD 14 – $\mathbf{a}_+$

K_+	K_0	$a_{+,0}$	$a_{+,1}$	$a_{+,2}$	$a_{+,3}$	$a_{+,4}$	$a_{+,5}$	$a_{+,6}$	$a_{+,7}$	$a_{+,8}$	$a_{+,9}$
2	2	0.0270(12)	-0.0792(49)	-	-	-	-	-	-	-	-
2	3	0.0273(13)	-0.0761(63)	-	-	-	-	-	-	-	-
3	2	0.0257(14)	-0.0805(49)	0.069(30)	-	-	-	-	-	-	-
3	3	0.0261(14)	-0.0728(64)	0.096(34)	-	-	-	-	-	-	-
3	4	0.0261(14)	-0.0728(76)	0.096(39)	-	-	-	-	-	-	-
4	3	0.0261(14)	-0.0729(68)	0.096(35)	0.008(90)	-	-	-	-	-	-
4	4	0.0261(14)	-0.0730(77)	0.091(62)	-0.02(20)	-	-	-	-	-	-
5	5	0.0262(15)	-0.0735(79)	0.084(67)	-0.03(19)	0.03(68)	-	-	-	-	-
6	6	0.0261(14)	-0.0735(79)	0.086(69)	-0.03(19)	-0.00(64)	0.01(65)	-	-	-	-
7	7	0.0262(14)	-0.0732(84)	0.088(69)	-0.02(18)	0.01(65)	0.02(73)	-0.03(70)	-	-	-
8	8	0.0261(14)	-0.0732(80)	0.089(72)	-0.02(18)	-0.00(66)	0.03(86)	-0.04(90)	0.03(73)	-	-
9	9	0.0261(14)	-0.0729(84)	0.095(75)	-0.02(19)	-0.04(68)	0.1(1.0)	-0.1(1.2)	0.1(1.1)	-0.06(79)	-
10	10	0.0261(14)	-0.0726(89)	0.101(79)	-0.01(20)	-0.09(73)	0.2(1.3)	-0.3(1.7)	0.2(1.8)	-0.2(1.4)	0.08(87)

HPQCD 14 – $\mathbf{a}_0$

K_+	K_0	$a_{0,0}$	$a_{0,1}$	$a_{0,2}$	$a_{0,3}$	$a_{0,4}$	$a_{0,5}$	$a_{0,6}$	$a_{0,7}$	$a_{0,8}$	$a_{0,9}$
2	2	0.0883(44)	-0.250(17)	-	-	-	-	-	-	-	-
2	3	0.0880(44)	-0.243(19)	0.052(65)	-	-	-	-	-	-	-
3	2	0.0907(46)	-0.240(17)	-	-	-	-	-	-	-	-
3	3	0.0906(44)	-0.215(22)	0.137(73)	-	-	-	-	-	-	-
3	4	0.0907(47)	-0.215(22)	0.14(11)	-0.01(31)	-	-	-	-	-	-
4	3	0.0907(45)	-0.214(22)	0.139(72)	-	-	-	-	-	-	-
4	4	0.0907(46)	-0.215(25)	0.12(19)	-0.08(60)	-	-	-	-	-	-
5	5	0.0909(46)	-0.218(25)	0.10(19)	-0.12(55)	0.04(63)	-	-	-	-	-
6	6	0.0907(45)	-0.217(25)	0.10(19)	-0.11(53)	0.06(66)	-0.02(66)	-	-	-	-
7	7	0.0907(46)	-0.217(26)	0.11(20)	-0.08(51)	0.03(73)	0.03(81)	-0.04(70)	-	-	-
8	8	0.0908(46)	-0.217(25)	0.11(20)	-0.08(50)	-0.01(84)	0.1(1.0)	-0.09(96)	0.08(74)	-	-
9	9	0.0907(46)	-0.215(25)	0.13(22)	-0.05(50)	-0.06(95)	0.2(1.4)	-0.2(1.5)	0.1(1.2)	-0.05(82)	-
10	10	0.0907(46)	-0.214(27)	0.15(24)	-0.03(49)	-0.2(1.1)	0.4(1.8)	-0.5(2.2)	0.4(2.1)	-0.3(1.6)	0.13(90)

Combine data

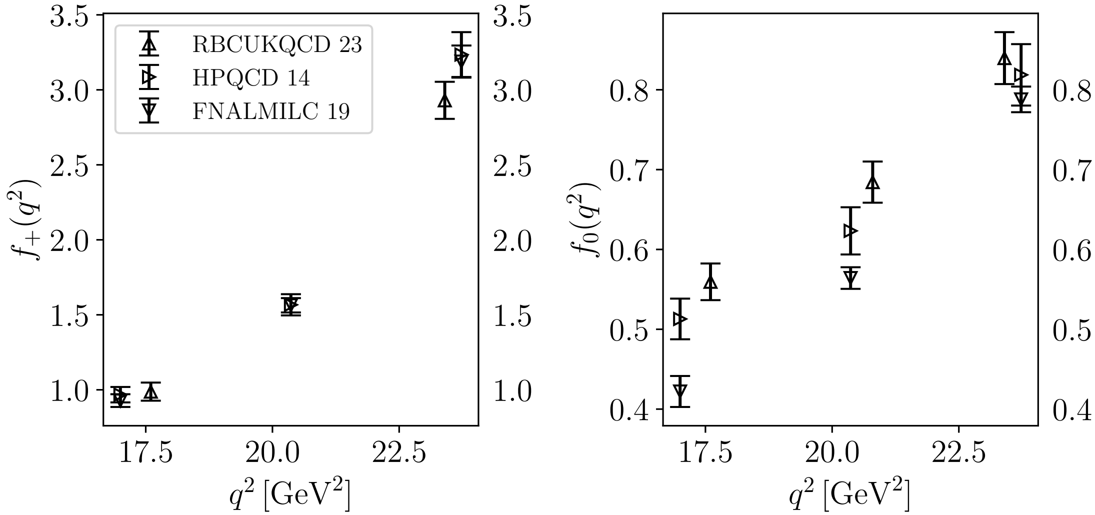

Combine lattice data

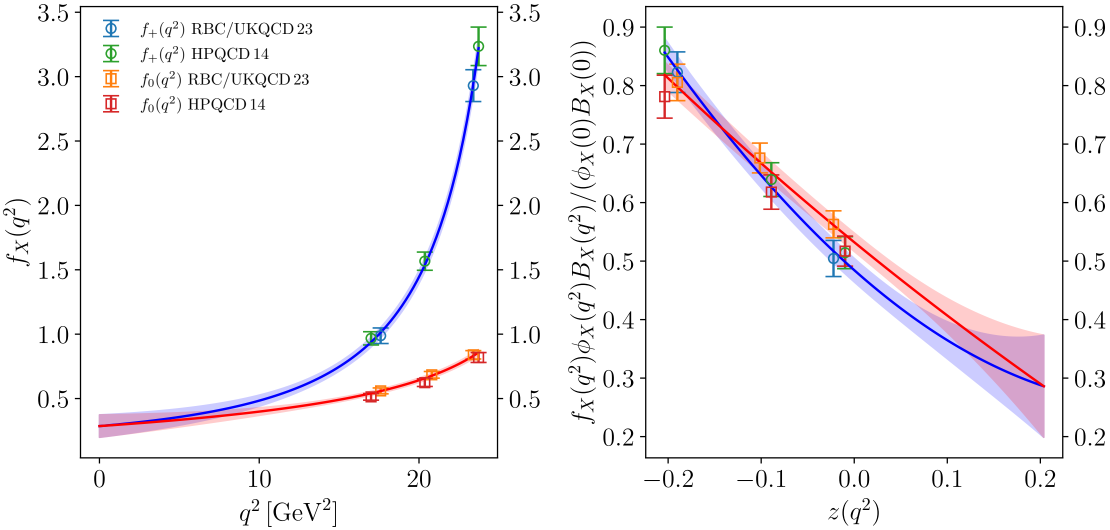

K_+	K_0	$a_{+,0}$	$a_{+,1}$	$a_{+,2}$	$a_{+,3}$	$a_{+,4}$	p	χ^2/N_{dof}	N_{dof}
2	2	0.02641(58)	−0.0824(26)				0.00	5.15	14
2	3	0.02668(68)	−0.0811(31)				0.00	5.50	13
3	2	0.02477(68)	−0.0829(26)	0.054(12)			0.00	3.95	13
3	3	0.02534(73)	−0.0792(31)	0.062(12)			0.00	3.89	12
3	4	0.02534(73)	−0.0781(34)	0.067(14)			0.00	4.19	11
4	3	0.02535(73)	−0.0776(38)	0.074(20)	0.023(30)		0.00	4.19	11
4	4	0.02592(97)	−0.033(50)	0.69(69)	2.1(2.3)		0.00	4.53	10
5	5	0.0266(10)	0.052(65)	2.21(97)	11.1(5.6)	17.2(15.1)	0.00	5.04	8

K_+	K_0	$a_{0,0}$	$a_{0,1}$	$a_{0,2}$	$a_{0,3}$	$a_{0,4}$	p	χ^2/N_{dof}	N_{dof}
2	2	0.0854(17)	−0.2565(75)				0.00	5.15	14
2	3	0.0856(18)	−0.2527(91)	0.021(27)			0.00	5.50	13
3	2	0.0858(18)	−0.2501(77)				0.00	3.95	13
3	3	0.0864(18)	−0.2379(95)	0.061(28)			0.00	3.89	12
3	4	0.0869(19)	−0.231(13)	0.067(29)	−0.08(10)		0.00	4.19	11
4	3	0.0869(19)	−0.229(15)	0.091(48)			0.00	4.19	11
4	4	0.0887(27)	−0.08(17)	2.2(2.4)	7.0(7.9)		0.00	4.53	10
5	5	0.0887(28)	0.07(20)	6.1(3.3)	41.5(19.0)	93.3(44.0)	0.00	5.04	8

Determining $|V_{ub}|$

Combining LHCb results [LHCb2021[28]] for

$$R_{\text{BF},[q^2_{\text{min}},q^2_{\text{max}}]} = \frac{\int_{q^2_{\text{min}}}^{q^2_{\text{max}}} \frac{d\mathcal{B}(B_s^0 \to K^- \mu^+ \nu_\mu)}{dq^2}}{\mathcal{B}(B_s^0 \to D_s^- \mu^+ \nu_\mu)}$$

in low ($q^2 \leq 7\,\text{GeV}^2$), high ($q^2 \geq 7\,\text{GeV}^2$) and combined bins

$$R_{\text{BF,low}} = 1.66(08)(09) \times 10^{-3}$$
$$R_{\text{BF,high}} = 3.25(21)(^{+18}_{-19}) \times 10^{-3}$$
$$R_{\text{BF,all}} = 4.89(21)(^{+24}_{-25}) \times 10^{-3}$$

and for [LHCb2020[29]]

$$\mathcal{B}(B_s^0 \to D_s^- \mu^+ \nu_\mu) = 2.49(12)(21) \times 10^{-2}$$

Find $|V_{ub}|$ from

$$|V_{ub}| = \sqrt{\frac{R_{\text{BF,bin}}\, \mathcal{B}(B_s^0 \to D_s^- \mu^+ \nu_\mu)}{\tau_{B_s^0}\, \Gamma_{0,\text{bin}}(B_s \to K \ell \nu)}}$$

where $\Gamma_{0,\text{bin}} = \Gamma_{\text{bin}}/|V_{ub}|^2$. Using RBC-UKQCD23 $(K_+, K_0) = (5, 5)$

$$|V_{ub}| = \begin{cases} 4.10(240) \times 10^{-3} & \text{low} \\ 3.76(55) \times 10^{-3} & \text{high} \\ 3.78(61) \times 10^{-3} & \text{all} \end{cases}$$

For comparison

$$|V_{ub}|^{\text{FLAG21}}_{\text{exclusive}} = 3.74(17) \times 10^{-3}$$ [1, 14, 30–34]

R ratios for LFU tests

$$R(P) = \frac{\int_{m_\tau^2}^{q^2_{\max}} dq^2 \, \frac{d\Gamma(B_{(s)}\to P\tau\bar{\nu}_\tau)}{dq^2}}{\int_{m_\ell^2}^{q^2_{\max}} dq^2 \, \frac{d\Gamma(B_{(s)}\to P\ell\bar{\nu}_\ell)}{dq^2}}$$

$$R^{\text{new}}(P) = \frac{\int_{q^2_{\min}}^{q^2_{\max}} dq^2 \, \frac{d\Gamma(B_{(s)}\to P\tau\bar{\nu}_\tau)}{dq^2}}{\int_{q^2_{\min}}^{q^2_{\max}} dq^2 \, \frac{\omega_\tau(q^2)}{\omega_\ell(q^2)} \frac{d\Gamma(B_{(s)}\to P\ell\bar{\nu}_\ell)}{dq^2}}$$

- Adopt idea proposed for $B_{(s)} \to V$ decays [Isidori–Sumensari[35]]
  - Common integration range; $q^2_{\min} \geq m_\tau^2$ [Freytsis et al[36], Bernlochner et al[37], Soni[38]]
  - *Same* weights for vector parts in integrands for τ and ℓ
- Write

$$\frac{d\Gamma(B_{(s)}\to P\ell\nu)}{dq^2} = \Phi\, \omega_\ell(q^2) \left[F_V^2 + (F_S^\ell)^2 \right]$$

$$\Phi = \eta \frac{G_F^2 |V_{xb}|^2}{24\pi^3}$$

$$\omega_\ell = \left(1 - \frac{m_\ell^2}{q^2}\right)^2 \left(1 + \frac{m_\ell^2}{2q^2}\right)$$

$$F_V^2 = \vec{k}^3 |f_+(q^2)|^2$$

$$(F_S^\ell)^2 = \frac{3}{4} |\vec{k}| \frac{m_\ell^2}{m_\ell^2 + 2q^2} \frac{(M^2 - m^2)^2}{M^2} |f_0(q^2)|^2$$

R ratios for LFU tests

$$R(P) = \frac{\int_{m_\tau^2}^{q^2_{max}} dq^2 \, \frac{d\Gamma(B_{(s)}\to P\tau\bar{\nu}_\tau)}{dq^2}}{\int_{m_\ell^2}^{q^2_{max}} dq^2 \, \frac{d\Gamma(B_{(s)}\to P\ell\bar{\nu}_\ell)}{dq^2}}$$

$$R^{new}(P) = \frac{\int_{q^2_{min}}^{q^2_{max}} dq^2 \, \frac{d\Gamma(B_{(s)}\to P\tau\bar{\nu}_\tau)}{dq^2}}{\int_{q^2_{min}}^{q^2_{max}} dq^2 \, \frac{\omega_\tau(q^2)}{\omega_\ell(q^2)} \frac{d\Gamma(B_{(s)}\to P\ell\bar{\nu}_\ell)}{dq^2}}$$

- Adopt idea proposed for $B_{(s)} \to V$ decays [Isidori–Sumensari[35]]
  - Common integration range; $q^2_{min} \geq m_\tau^2$ [Freytsis et al[36], Bernlochner et al[37], Soni[38]]
  - *Same* weights for vector parts in integrands for τ and ℓ
- Write

$$\frac{d\Gamma(B_{(s)}\to P\ell\nu)}{dq^2} = \Phi \, \omega_\ell(q^2) \left[F_V^2 + (F_S^\ell)^2\right]$$

- If drop scalar contribution, $(F_S^\ell)^2$, in denominator ($m_\ell^2/2q^2 \leq m_\mu^2/2m_\tau^2 = 0.002$) expect

$$R^{new,SM}(P) = 1 + \frac{\int_{q^2_{min}}^{q^2_{max}} dq^2 \, \omega_\tau(q^2)(F_S^\tau)^2}{\int_{q^2_{min}}^{q^2_{max}} dq^2 \, \omega_\tau(q^2) F_V^2}$$

References I

[1] JM Flynn et al. (RBC, UKQCD), $B \to \pi \ell \nu$ and $B_s \to K \ell \nu$ form factors and $|V_{ub}|$ from 2+1-flavor lattice QCD with domain-wall light quarks and relativistic heavy quarks, Phys. Rev. D **91**, 074510 (2015), arXiv:1501.05373 [hep-lat].

[2] S Okubo, Exact bounds for k-l-3 decay parameters, Phys. Rev. D **3**, 2807–2813 (1971).

[3] S Okubo, New improved bounds for k-l-3 parameters, Phys. Rev. D **4**, 725–733 (1971).

[4] S Okubo and IF Shih, Exact inequality and test of chiral sw(3) theory in k-l-3 decay problem, Phys. Rev. D **4**, 2020–2029 (1971).

[5] C Bourrely et al., Semileptonic Decays of Pseudoscalar Particles ($M \to M' \ell \nu_\ell$) and Short Distance Behavior of Quantum Chromodynamics, Nucl. Phys. B **189**, 157–181 (1981).

[6] CG Boyd et al., Model independent extraction of |V(cb)| using dispersion relations, Phys. Lett. B **353**, 306–312 (1995), arXiv:hep-ph/9504235.

[7] CG Boyd et al., Model independent determinations of $\bar{B} \to D \ell \bar{\nu}$, $D^* \ell \bar{\nu}$ form-factors, Nucl. Phys. B **461**, 493–511 (1996), arXiv:hep-ph/9508211.

[8] CG Boyd et al., Precision corrections to dispersive bounds on form-factors, Phys. Rev. D **56**, 6895–6911 (1997), arXiv:hep-ph/9705252.

[9] L Lellouch, Lattice constrained unitarity bounds for anti-B0 —> pi+ lepton- anti-lepton-neutrino decays, Nucl. Phys. B **479**, 353–391 (1996), arXiv:hep-ph/9509358.

References II

[10] N Gubernari et al., Non-local matrix elements in $B_{(s)} \longrightarrow \{K^{(*)}, \phi\}\ell^+\ell^-$, JHEP **02**, 088 (2021), arXiv:2011.09813 [hep-ph].

[11] N Gubernari et al., Improved theory predictions and global analysis of exclusive $b \longrightarrow s\mu^+\mu^-$ processes, JHEP **09**, 133 (2022), arXiv:2206.03797 [hep-ph].

[12] T Blake et al., Dispersive bounds for local form factors in $\Lambda_b \longrightarrow \Lambda$ transitions, (2022), arXiv:2205.06041 [hep-ph].

[13] JM Flynn et al., Bayesian inference for form-factor fits regulated by unitarity and analyticity, (2023), arXiv:2303.11285 [hep-ph].

[14] JA Bailey et al. (Fermilab Lattice, MILC), $|V_{ub}|$ from $B \longrightarrow \pi\ell\nu$ decays and (2+1)-flavor lattice QCD, Phys. Rev. D **92**, 014024 (2015), arXiv:1503.07839 [hep-lat].

[15] A Bazavov et al. (Fermilab Lattice, MILC), $B_s \longrightarrow K\ell\nu$ decay from lattice QCD, Phys. Rev. D **100**, 034501 (2019), arXiv:1901.02561 [hep-lat].

[16] G Martinelli et al., Exclusive semileptonic $B \longrightarrow \pi\ell\nu_\ell$ and $B_s \longrightarrow K\ell\nu_\ell$ decays through unitarity and lattice QCD, (2022), arXiv:2202.10285 [hep-ph].

[17] CM Bouchard et al. (HPQCD), $B_s \longrightarrow K\ell\nu$ form factors from lattice QCD, Phys. Rev. D **90**, 054506 (2014), arXiv:1406.2279 [hep-lat].

[18] M Di Carlo et al., Unitarity bounds for semileptonic decays in lattice QCD, Phys. Rev. D **104**, 054502 (2021), arXiv:2105.02497 [hep-lat].

References III

[19] G Martinelli et al., Constraints for the semileptonic B→D(*) form factors from lattice QCD simulations of two-point correlation functions, Phys. Rev. D **104**, 094512 (2021), arXiv:2105.07851 [hep-lat].

[20] G Martinelli et al., $|V_{cb}|$ and $R(D)^{(*)}$) using lattice QCD and unitarity, Phys. Rev. D **105**, 034503 (2022), arXiv:2105.08674 [hep-ph].

[21] G Martinelli et al., |Vcb|, lepton flavor universality and SU(3)F symmetry breaking in Bs→Ds(*)$\ell\nu\ell$ decays through unitarity and lattice QCD, Phys. Rev. D **106**, 093002 (2022), arXiv:2204.05925 [hep-ph].

[22] JM Flynn et al., Exclusive semileptonic $B_s \to K\ell\nu$ decays on the lattice, (2023), arXiv:2303.11280 [hep-lat].

[23] A Khodjamirian and AV Rusov, $B_s \to K\ell\nu_\ell$ and $B_{(s)} \to \pi(K)\ell^+\ell^-$ decays at large recoil and CKM matrix elements, JHEP **08**, 112 (2017), arXiv:1703.04765 [hep-ph].

[24] B Colquhoun et al. (JLQCD), Form factors of $B \to \pi\ell\nu$ and a determination of $|V_{ub}|$ with Möbius domain-wall fermions, Phys. Rev. D **106**, 054502 (2022), arXiv:2203.04938 [hep-lat].

[25] R Glattauer et al. (Belle), Measurement of the decay $B \to D\ell\nu_\ell$ in fully reconstructed events and determination of the Cabibbo-Kobayashi-Maskawa matrix element $|V_{cb}|$, Phys. Rev. D **93**, 032006 (2016), arXiv:1510.03657 [hep-ex].

[26] D Simons et al., Self-consistent optimization of the z-Expansion for B meson decays, (2023), arXiv:2304.13045 [hep-ph].

References IV

[27] C Bourrely et al., Model-independent description of $B \to \pi \ell \nu$ decays and a determination of $|V_{ub}|$, Phys. Rev. D **79**, [Erratum: Phys.Rev.D 82, 099902 (2010)], 013008 (2009), arXiv:0807.2722 [hep-ph].

[28] R Aaij et al. (LHCb), First observation of the decay $B_s^0 \to K^- \mu^+ \nu_\mu$ and Measurement of $|V_{ub}|/|V_{cb}|$, Phys. Rev. Lett. **126**, 081804 (2021), arXiv:2012.05143 [hep-ex].

[29] R Aaij et al. (LHCb), Measurement of $|V_{cb}|$ with $B_s^0 \to D_s^{(*)-} \mu^+ \nu_\mu$ decays, Phys. Rev. D **101**, 072004 (2020), arXiv:2001.03225 [hep-ex].

[30] P del Amo Sanchez et al. (BaBar), Study of $B \to \pi \ell \nu$ and $B \to \rho \ell \nu$ Decays and Determination of $|V_{ub}|$, Phys. Rev. D **83**, 032007 (2011), arXiv:1005.3288 [hep-ex].

[31] JP Lees et al. (BaBar), Branching fraction and form-factor shape measurements of exclusive charmless semileptonic B decays, and determination of $|V_{ub}|$, Phys. Rev. D **86**, 092004 (2012), arXiv:1208.1253 [hep-ex].

[32] H Ha et al. (Belle), Measurement of the decay $B^0 \to \pi^- \ell^+ \nu$ and determination of $|V_{ub}|$, Phys. Rev. D **83**, 071101 (2011), arXiv:1012.0090 [hep-ex].

[33] A Sibidanov et al. (Belle), Study of Exclusive $B \to X_u \ell \nu$ Decays and Extraction of $\|V_{ub}\|$ using Full Reconstruction Tagging at the Belle Experiment, Phys. Rev. D **88**, 032005 (2013), arXiv:1306.2781 [hep-ex].

[34] Y Aoki et al. (Flavour Lattice Averaging Group (FLAG)), FLAG Review 2021, Eur. Phys. J. C **82**, 869 (2022), arXiv:2111.09849 [hep-lat].

References V

[35] G Isidori and O Sumensari, Optimized lepton universality tests in $B \longrightarrow V\ell\bar{\nu}$ decays, Eur. Phys. J. C **80**, 1078 (2020), arXiv:2007.08481 [hep-ph].

[36] M Freytsis et al., Flavor models for $\bar{B} \longrightarrow D^{(*)}\tau\bar{\nu}$, Phys. Rev. D **92**, 054018 (2015), arXiv:1506.08896 [hep-ph].

[37] FU Bernlochner and Z Ligeti, Semileptonic $B_{(s)}$ decays to excited charmed mesons with e, μ, τ and searching for new physics with $R(D^{**})$, Phys. Rev. D **95**, 014022 (2017), arXiv:1606.09300 [hep-ph].

[38] JM Flynn et al. (RBC, UKQCD), Nonperturbative calculations of form factors for exclusive semileptonic $B_{(s)}$ decays, PoS **ICHEP2020**, 436 (2021), arXiv:2012.04323 [hep-ph].